SPEED SENSORLESS FIELD-ORIENTED CONTROL OF INDUCTION MOTORS WITH AN IMPROVED FLUX ESTIMATOR

Myoung-Ho Shin*, Dong-Seok Hyun*, Soon-Bong Cho**, Song-Yul Choe***
* Dept. of Electrical Engineering Hanyang University
** Dept. of Electrical Engineering Doowon Technical College
*** Hyundai Precision & Ind. Co., Ltd.
Address : Dept. of Electrical Engineering Hanyang University, Seongdong-ku, 133-791, Seoul, Korea
E-mail : dshyun@hyunp1.hanyang.ac.kr

Abstract- This paper proposes a programmable low pass filter(LPF) to estimate stator flux for speed sensorless stator flux orientation control of induction motors. The programmable LPF is developed to solve the dc drift problem associated with a pure integrator and a LPF with fixed pole. The pole of the programmable LPF is located far from the origin to decrease the time constant as speed increases. The programmable LPF has the phase and the magnitude compensator to exactly estimate stator flux in a wide speed range. So, the drift problem is much improved and the stator flux is exactly estimated in the wide speed range.

1. INTRODUCTION

Recently, induction motors have been used more in the industrial variable speed drive system with the development of the vector control technology. This method needs a speed sensor such as a shaft encoder for speed control. However, a speed sensor cannot be mounted in some cases, such as motor drives in a hostile environment, high-speed drives, etc., and also need careful cabling arrangements with attention to electrical noise. Moreover, it makes the price of the system expensive and the motor size bulky. Recently several speed sensorless vector control schemes have been proposed [1]-[7].

The stator flux for speed sensorless vector control is estimated by the integration of the back emf. The integration of back emf by pure integrator has the drift and the saturation problem by the initial condition and the dc offset. So, pure integrator is replaced by an analog low pass filter(LPF) [2]. However, it has a very low cutting frequency to operate in a wide speed range. So, there still remains the drift problem due to the very large time constant of the LPF. Many efforts have been made to solve the problem [3]-[5].

This paper proposes a programmable LPF with the phase and the magnitude compensator to exactly estimate the stator flux in a wide speed range. The pole of the programmable LPF is located far from the origin in order to decrease the time constant as the speed increases. So, the stator flux is exactly estimated and the drift problem is much improved by the small time constant in a wide speed range. The proposed programmable LPF is used in speed sensorless stator flux orientation induction motor drive [7]. Simulation and experimental results confirm the effectiveness of the proposed programmable LPF.

2. DESCRIPTION OF PROGRAMMABLE LPF

The principle of programmable LPF method of integration can be explained as follows.

In the stationary α-β reference frame, the stator flux is given by

$$\lambda_s = \int (v_s - R_s i_s) dt \tag{1}$$

where v_s = stator voltage, R_s = stator resistance, i_s = stator current.

The integration of (1) by pure integrator(1/s) has the drift and the saturation problem. So, the integration by pure integrator is replaced by LPF. The estimated stator flux by LPF can be given as

$$\frac{\hat{\lambda}_{sl}}{v_e} = \frac{1}{s+a} \tag{2}$$

where '^' = estimated value, $\hat{\lambda}_{sl}$ = estimated stator flux by LPF, a = pole, v_e = back emf$(v_s - R_s i_s)$.

The phase lag and gain of (2) can be given, respectively, as

$$\hat{\phi} = -\tan^{-1}\left(\frac{\hat{\omega}_e}{a}\right) \tag{3}$$

$$\hat{M} = \left| \frac{\hat{\lambda}_{sl}}{v_e} \right| = \frac{1}{\sqrt{\hat{\omega}_e^2 + a^2}} \quad (4)$$

where

$\hat{\omega}_e$ = angular frequency.

Fig. 1 shows the phase lag of $\hat{\lambda}_{sl}$ estimated by the LPF, and the phase lag of $\hat{\lambda}_s$ estimated by the pure integrator. The phase lag of $\hat{\lambda}_s$ is 90° and the gain is $1/|\hat{\omega}_e|$. For the exact estimation of the stator flux, the phase lag and the gain of $\hat{\lambda}_{sl}$ in (2) have to be, respectively, 90° and $1/|\hat{\omega}_e|$. And also, the LPF in (2) has very low cutting frequency to operate in a wide speed range. So, there still remains the drift problem due to very large time constant of the LPF.

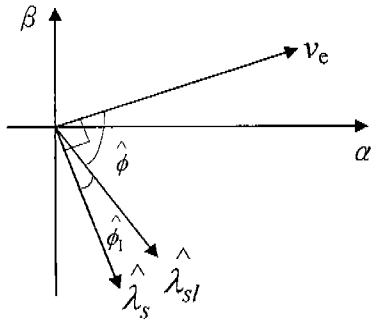

Fig. 1 Vector diagram of LPF and pure integrator.

In this paper, the gain is compensated by the gain compensator, $\hat{G}$ in (5) and the phase lag is compensated by the phase compensator, $\hat{P}$ in (6). Therefore, the new integrator with the gain and the phase compensator can be given as (7).

$$\hat{G} = \frac{\sqrt{\hat{\omega}_e^2 + a^2}}{|\hat{\omega}_e|} \quad (5)$$

$$\hat{P} = \exp(-j\hat{\phi}_1) \quad (6)$$

$$\frac{\hat{\lambda}_s}{v_e} = \frac{1}{(s+a)} \frac{\sqrt{\hat{\omega}_e^2 + a^2}}{|\hat{\omega}_e|} \exp(-j\hat{\phi}_1) \quad (7)$$

The cutting frequency has to be high to solve the drift problem due to very large time constant. But, in that case, flux estimation is poor somewhat in very low speed range. So, in this paper, the pole a is selected as (8) as a function of frequency.

$$a = \frac{|\hat{\omega}_e|}{k} \quad (8)$$

where k = constant.

So, the time constant of the programmable LPF, $(1/a) = k/|\hat{\omega}_e|$ is decreased with the increase of the speed. Therefore, the complete expression for stator flux estimator can be derived as

$$\frac{\hat{\lambda}_s}{v_e} = \frac{1}{(s+|\hat{\omega}_e|/k)} \frac{\sqrt{\hat{\omega}_e^2 + (\hat{\omega}_e/k)^2}}{|\hat{\omega}_e|} \exp(-j\hat{\phi}_1) \quad (9)$$

where

$$\exp(-j\hat{\phi}_1) = \cos(\hat{\phi}_1) - j\sin(\hat{\phi}_1)$$

$$\cos(\hat{\phi}_1) = \frac{|\hat{\omega}_e|}{\sqrt{\hat{\omega}_e^2 + (\hat{\omega}_e/k)^2}}$$

$$\sin(\hat{\phi}_1) = \frac{\hat{\omega}_e/k}{\sqrt{\hat{\omega}_e^2 + (\hat{\omega}_e/k)^2}}$$

Fig. 2 shows the block diagram of the programmable LPF.

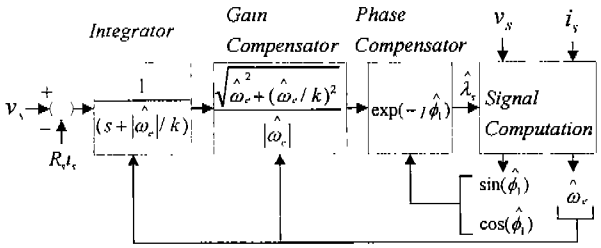

Fig. 2 Block diagram of the programmable LPF.

3. A DIRECT STATOR FLUX ORIENTATION SYSTEM

The control scheme of the proposed drive system is speed sensorless stator flux orientation. Fig. 3 shows the control block diagram of speed sensorless stator flux orientation control drive that incorporates the proposed programmable LPF. The stator flux magnitude and the transformation angle can be written as follows from the flux in stationary α-β reference frame.

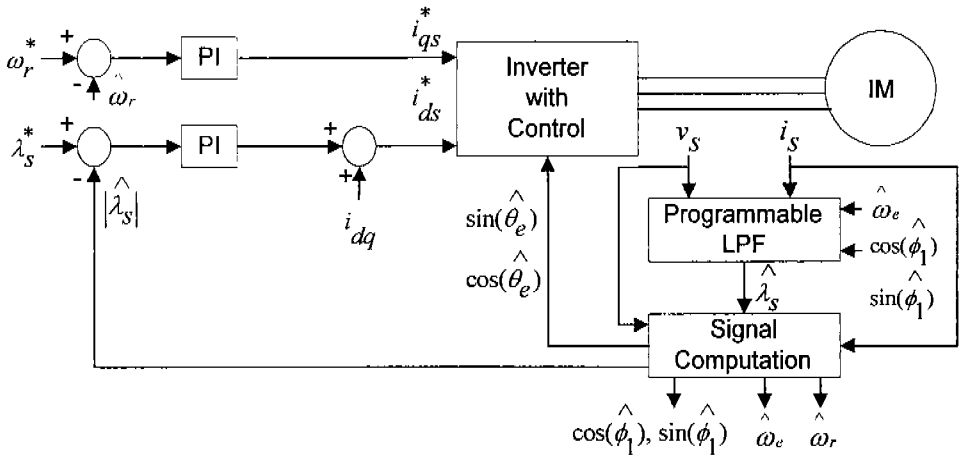

Fig. 3 Block diagram of speed sensorless stator flux orientation control drive.

$$|\hat{\lambda}_s| = \sqrt{\hat{\lambda}_{\alpha s}^2 + \hat{\lambda}_{\beta s}^2} \tag{10}$$

$$\cos(\hat{\theta}) = \frac{\hat{\lambda}_{\alpha s}}{|\hat{\lambda}_s|} \tag{11}$$

$$\sin(\hat{\theta}) = \frac{\hat{\lambda}_{\beta s}}{|\hat{\lambda}_s|} \tag{12}$$

The estimated slip speed and the decoupling compensator is represented in rotating d-q reference frame as follows [7].

$$\hat{\omega}_{sl} = \frac{(1+\sigma\tau_r p)L_s i_{qs}}{\tau_r(\lambda_{ds} - \sigma L_s i_{ds})} \tag{13}$$

$$i_{dq} = \frac{\hat{\omega}_{sl}\,\tau_r \sigma i_{qs}}{(1+\sigma\tau_r p)} \tag{14}$$

where

$\sigma = (1 - \frac{L_m^2}{L_s L_r})$: total leakage factor

$\tau_r = L_r / R_r$: rotor time constant

L_m : magnetizing inductance

L_s, L_r : stator and rotor inductance

$p = d/dt$: differential operator

The synchronous speed and the rotor speed can be given as

$$\hat{\omega}_e = \frac{((v_{\beta s} - R_s i_{\beta s})\hat{\lambda}_{\alpha s} - (v_{\alpha s} - R_s i_{\alpha s})\hat{\lambda}_{\beta s})}{|\hat{\lambda}_s|^2} \tag{15}$$

$$\hat{\omega}_r = \hat{\omega}_e - \hat{\omega}_{sl} \tag{16}$$

When the slip in (13) and decoupling compensation current (14) are calculated, a differentiator is very sensitive to the noise. So, the derivative term is eliminated and steady-state form is used.

The control system may be unstable due to the very high peak components included in slip in (13). To make the system stable, a limiter is used to limit the very high peak components. The error included in the rotor speed is removed by the use of low pass filter.

The stator voltage is reconstructed from the inverter switching states. The algorithm of the stator voltage estimation is as follows [8]. A switching function SA for phase A is 1 when upper switch of phase A is on. SA is 0 when lower switch of phase A is on. A similar definition is adopted for phase B and C. The stator phase voltages can be given in terms of switching states and the dc link voltage as follows.

$$v_{as} = \frac{V_{dc}}{3}(2SA - SB - SC) \tag{17-a}$$

$$v_{bs} = \frac{V_{dc}}{3}(-SA + 2SB - SC) \tag{17-b}$$

$$v_{cs} = \frac{V_{dc}}{3}(-SA - SB + 2SC) \tag{17-c}$$

Applying the 3 to 2 phase transformation to (17), stator voltage in stationary α-β reference frame can be given as

$$v_{\alpha s} = \frac{V_{dc}}{3}(2SA - SB - SC) \tag{18-a}$$

$$v_{\beta s} = \frac{V_{dc}}{\sqrt{3}}(SB - SC) \qquad (18\text{-b})$$

The processor reads the outputs of prefilter(s= -2985) through an A/D converter. The signal aliasing is prevented by the prefilter. The phase lag and the reduction of magnitude caused by the prefilter can be neglected because the pole of the prefilter is located so far from the origin.

4. SIMULATION RESULTS

The proposed programmable LPF was studied by simulation with the drive system shown in Fig. 3. ACSL(Advanced Continuous Simulation Language) was used for simulation. The constant k in (9) is selected as 3 for good performance of the drive by trial and error. The lower limit of $a(=|\hat{\omega}_e|/k)$ is 1 to prevent the time constant of the programmable LPF from being much increased when the rotor speed is close to 0[rpm]. The motor parameters are shown in Table 1.

TABLE 1
INDUCTION MOTOR PARAMETERS

Parameter	Value	
Rated power	2.2	[kW]
Pole number	4	
Magnetizing current(peak)	5	[A]
Rated flux	0.25	[Wb]
Stator resistance	1.26	[Ω]
Rotor resistance	0.2	[Ω]
Magnetizing inductance	50	[mH]
Moment of inertia	0.017	[kg·m^2]
Stator leakage inductance	4.7	[mH]
Rotor leakage inductance	4.7	[mH]

Fig. 4 shows the speed and the flux waveforms with the LPF in (2) with fixed pole(s=-1). Because the pole is close to the origin, the flux and the speed estimation are unstable due to the large time constant of the LPF when the speed is changed from 1500 to 400[rpm]. Fig. 4(a) shows that the estimated speed is delayed by the use of a low pass filter to remove high frequency components involved in the estimated speed. Fig. 4(d) shows that the LPF produces flux estimation error when the speed is changed.

Fig. 5 shows speed and flux waveforms with the proposed programmable LPF. Because the pole of the programmable LPF is located far from the origin, it can be seen that the speed and the flux estimation are stable when the speed is changed. Fig. 5(d) shows the time constant of the programmable LPF. The time constant of the programmable LPF varies between 0.0095 and 0.045. Fig. 5(e) shows that the stator flux is exactly estimated.

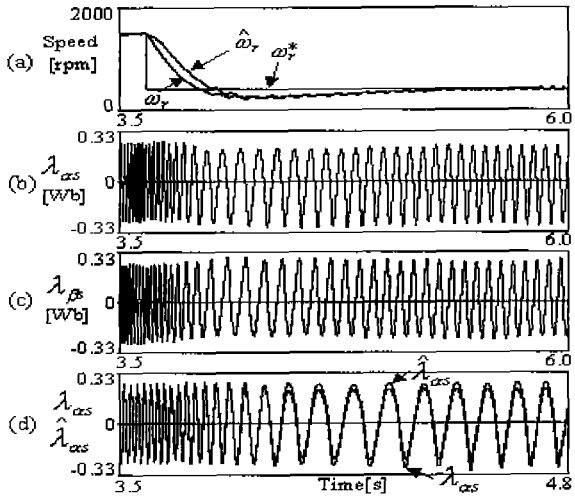

Fig. 4 Step response with LPF with fixed pole(s=-1).
(load torque : 6 [Nm], speed reference(ω_r^*) : 1500 → 400[rpm])

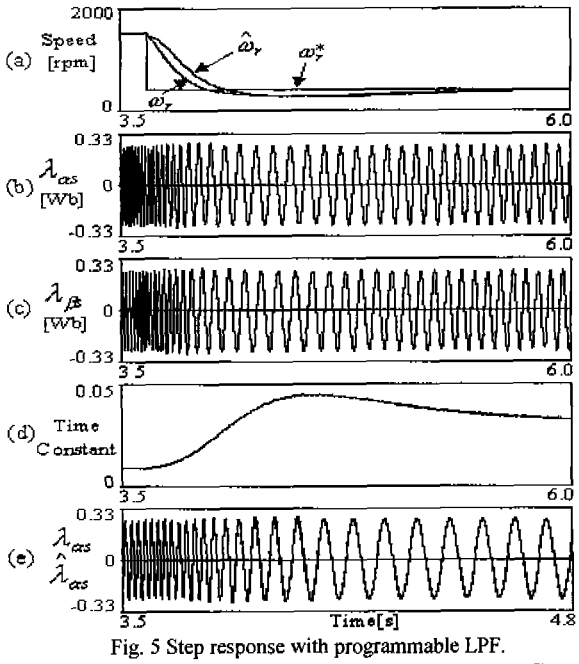

Fig. 5 Step response with programmable LPF.
(load torque : 6[Nm], speed reference : 1500 → 400[rpm])

5. EXPERIMENTAL RESULTS

In order to verify the proposed programmable LPF, the control system is implemented by the software of DSP TMS320C31. The inverter input voltage is V_{dc}=300[V]. The switching frequency is 5[kHz]. The current control period is T_c=100[μs]. The speed control period is T_s=1[ms]. The stator currents are detected through Hall-type sensors. The stator currents are sampled and held at every sampling instant, then A/D converted with 2[μs] conversion time. The lower limit of pole a is 1. The motor is 2.2[kW] three-phase induction motor shown in Table I .

When the motor speed is close to zero, the value of gain compensator in (9) becomes very large. The value is very

significantly affected by the small detuning of stator resistance. And the flux control at very low speed close to zero can be unstable. To avoid the unstability, the lower limit value of synchronous frequency in (9) is set at 3[rad/s].

The flux control loop acts at a wide speed range(including zero speed). When the flux control loop acted, the flux control was unstable. However, the unstability was able to be avoided by the use of small stator resistance(about 1.1 [Ω]) for the estimation of stator flux(the measured stator resistance is 1.26[Ω]). So, the flux control was able to be stable at zero speed. Voltage drop of stator resistance can be negligible as speed increases.

Fig. 6 shows the speed and the flux waveforms with the LPF with fixed pole(s=-20). Because the LPF does not have the pole close to origin, the speed and the flux estimation are unstable when the speed reference is zero.

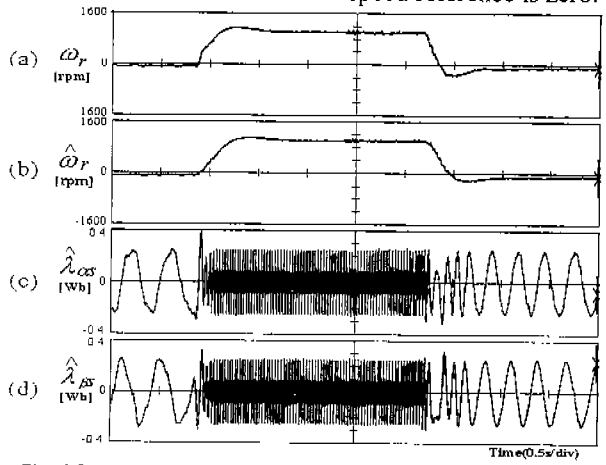

Fig. 6 Speed and flux waveforms with LPF with fixed pole(s=-20).
(no load, speed reference : 0 → 1000 → 0[rpm])

Fig. 7 shows the speed and the flux waveforms with the LPF with fixed pole(s=-1). Because the pole is close to the origin, the flux and the speed estimation are unstable due to the large time constant of the LPF when the speed is changed.

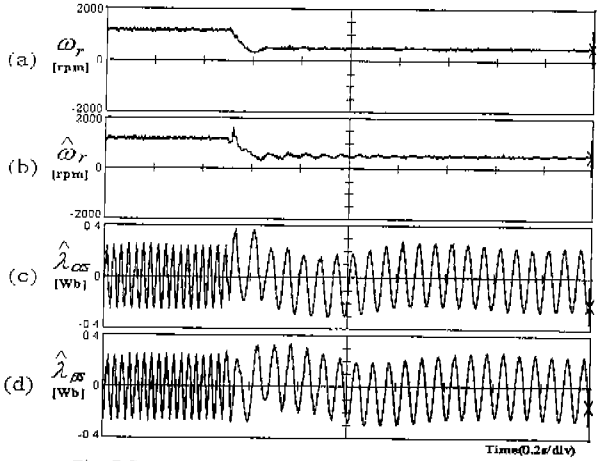

Fig. 7 Step response with LPF with fixed pole(s=-1).
(load torque : 4[Nm], speed reference : 1200 → 500[rpm])

Fig. 8 shows the speed and the flux waveforms with the proposed programmable LPF. It can be seen that because the programmable LPF has the pole farther from the origin, the speed and the flux estimation are stable when the speed is changed.

Fig. 9 shows zero speed start up characteristics with the proposed programmable LPF. The speed and the flux estimation are stable at zero speed compared with Fig. 6. Fig. 9(d) shows the variation of the pole of the programmable LPF between 14 and 1(lower limit value of the pole) when the speed is changed.

Fig. 10 shows speed reversal characteristics with the proposed programmable LPF. The speed reference is changed from -1500 to 1500[rpm]. Fig. 10(d) shows that the pole of programmable LPF varies between 104.7 and 1. The dc drift can seldom be seen.

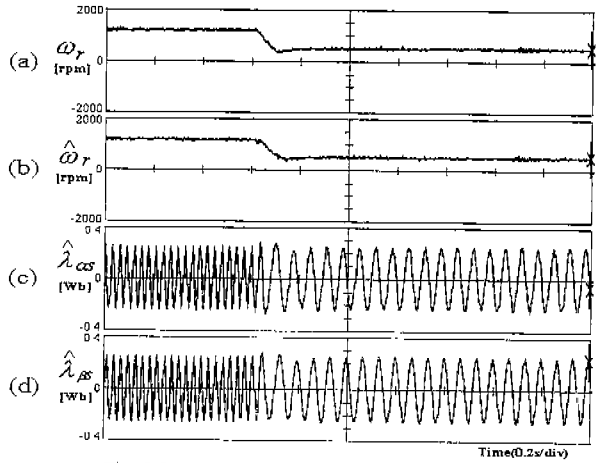

Fig. 8 Step response with programmable LPF.
(k=3, load torque : 4[Nm], speed reference : 1200 → 500[rpm])

Fig. 11 shows the locus of stator flux vector with the LPF with fixed pole(s=-1). The magnitude of the stator flux vector is not constant due to the dc drift.

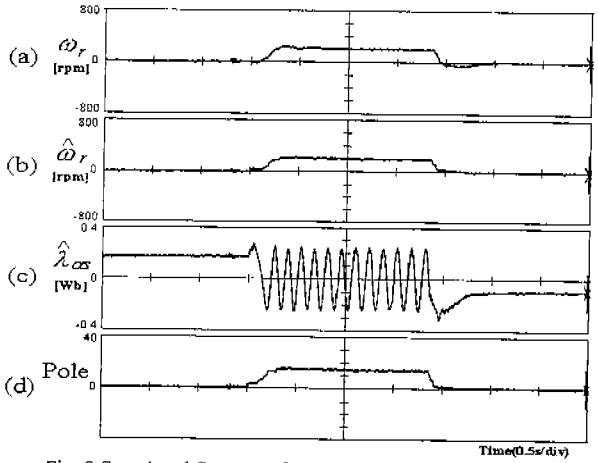

Fig. 9 Speed and flux waveforms with programmable LPF.
(k=3, no load, speed reference : 0 → 200 → 0[rpm])

Fig. 12 shows the locus of the stator flux vector with the programmable LPF. The magnitude of stator flux vector

remained nearly constant while the speed is changed from 1000 to 500[rpm].

6. CONCLUSION

This paper investigated the drift problem of stator flux estimated by the LPF with fixed pole due to the large time constant of the LPF, and proposed a programmable LPF to solve the drift problem.

The stator flux was exactly estimated with the phase and the magnitude compensator of the proposed programmable LPF in a wide speed range. And the drift problem was much improved by the small time constant of the programmable LPF. So, the speed sensorless drive system with the proposed programmable LPF was able to be more stable than the system with the LPF with fixed pole. The simulation and the experimental results have confirmed the proposed programmable LPF.

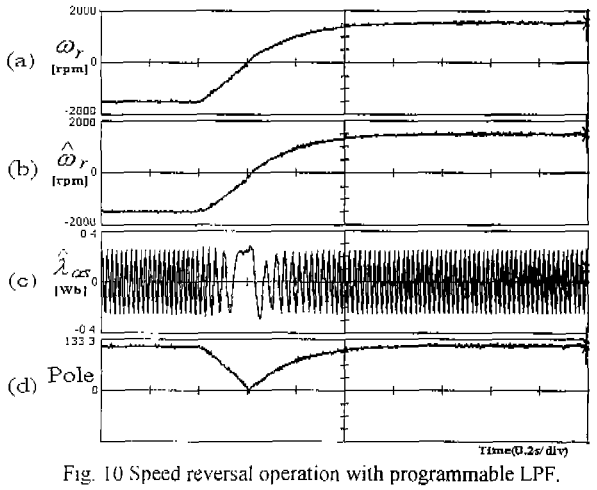

Fig. 10 Speed reversal operation with programmable LPF.
(k=3, no load, speed reference : -1500 → 1500[rpm])

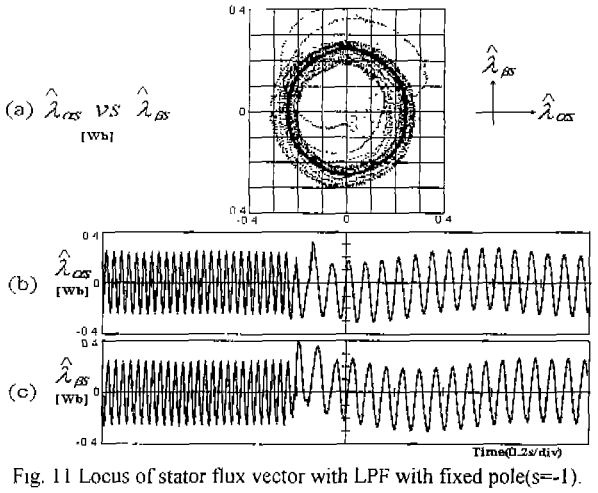

Fig. 11 Locus of stator flux vector with LPF with fixed pole(s=-1).
(load torque : 4[Nm], speed reference : 1000 → 500[rpm])

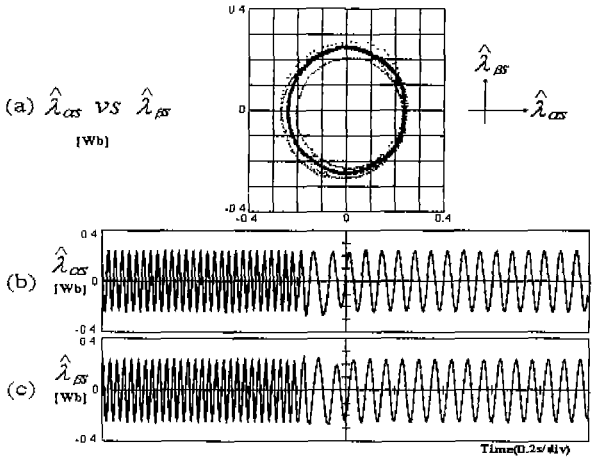

Fig. 12 Locus of stator flux vector with programmable LPF.
(k=3, load torque : 4[Nm], speed reference : 1000 → 500[rpm])

REFERENCES

[1] Xingyi Xu and Donald W. Novotny, "Implementation of Direct Stator Flux Orientation Control on a Versatile DSP Based System," *IEEE Trans. Indus. Appli.*, vol 27, no.4, pp. 694-700, 1991.

[2] Lazhar Ben-Brahim and Atsuo Kawamura, "A Fully Digitized Field-Oriented Controlled Induction Motor Drive Using Only Current Sensors," *IEEE Trans. Indus. Electron.*, vol. 39, no.3, pp.241-249,June 1992.

[3] George John, William Erdman, Raymond Hudson, ChiSheng Fan and Shailendra Mahajan, "Stator Flux Estimation from Inverter Switching States for the Field Oriented Control of Induction Generators," *IEEE IAS Ann. Mtg.*, pp.182-188, 1995.

[4] Bimal K. Bose and M. Godoy Simões, "Speed Sensorless Hybrid Vector Controlled Induction Motor Drive," *IEEE IAS Ann. Mtg.*, pp.137-143, 1995.

[5] Bimal K. Bose and Nitin R. Patel, "A Programmable Cascaded Low-Pass Filter-Based Flux Synthesis for a Stator Flux-Oriented Vector-Controlled Induction Motor Drive," *IEEE Trans. Indus. Electron.*, vol. 44, no.1, pp.140-143, February 1997.

[6] J. HU and B. WU, "New Integration Algorithms for Estimating Motor Flux Over a Wide Speed Range," *IEEE PESC'97*, pp.1075-1081, 1997.

[7] Xingyi Xu, Rik De Doncker and Donald W. Novotny, "A Stator Flux Oriented Induction Machine Drive," *IEEE Power Electron. Specialists Conf.* pp. 870-876, 1988.

[8] T. G. Habetler and D. M. Divan, "Control Strategies for Direct Torque Control Using Discrete Pulse Modulation," in *Proc. IEEE IAS Ann. Meet.*, Oct. 1989, pp. 514-522